Mixed columnar-plaquette crystal of correlated fermions on the two-dimensional pyrochlore lattice at fractional filling

F. Trousselet and D. Poilblanc
Laboratoire de Physique Théorique, CNRS, Université Paul Sabatier, 31062 Toulouse, France

R. Moessner
Max-Planck-Institut für Physik Komplexer Systeme, 01187 Dresden, Germany

(Received 29 June 2008; revised manuscript received 23 September 2008; published 3 November 2008)

We study a model of strongly correlated $S=1/2$ fermions on the planar pyrochlore, or checkerboard, lattice, at fractional (1/8) filling. Starting with the extended Hubbard model in the limit of strong Coulomb repulsion, low-energy configurations can be mapped onto hard-core dimer configurations whose dimers carry a spin degree of freedom. An effective Hamiltonian similar to the kinetic term of a quantum dimer model on the square lattice which rotates two parallel dimers (in a spin-singlet configuration) by 90° naturally emerges. We also introduce an additional term in the Hamiltonian, a generalized dimer plaquette interaction, in order to realize a closer analogy to the latter model. For a strong dimer plaquette attraction stabilizing a columnar phase, a spontaneous dimerization takes place in the direction of the columns of (spin-carrying) dimers. Using exact diagonalizations of two-dimensional periodic clusters, the analysis of the low-energy spectrum and of several types of correlation functions gives indeed evidence for a new type of lattice symmetry breaking phase, the eightfold degenerate mixed columnar-plaquette crystal, and for a transition from this phase to a resonating singlet-pair crystal (found in previous studies) which restores the rotational symmetry of the lattice. Similar conclusions and phase diagram are also reached from a simple variational approach.

DOI: 10.1103/PhysRevB.78.195101 PACS number(s): 71.10.Fd, 71.10.Hf

I. MODEL, PURPOSES, AND METHOD

A. Introduction and summary of previous results

The interplay between electronic correlations and the lattice geometry in quantum magnets can lead to a rich variety of spin gapped disordered phases, either spin liquids with fractionalized excitations or various types of valence-bond crystals (VBC), which break spontaneously some of the lattice symmetries. Among materials magnetically frustrated and possibly presenting such phases, those with a pyrochlore structure, a three-dimensional (3D) array of corner-sharing tetrahedra, are of particular interest because of the absence of magnetic order down to very low temperatures.[1] On a two-dimensional (2D) version of the pyrochlore lattice, the *checkerboard* lattice (see Fig. 1), the Heisenberg model presents a VBC of particular interest, the *plaquette* phase,[2] which exhibits the rotational symmetry of the lattice. To understand the physics of undoped and doped frustrated magnets and predict the occurrence of these phases in real materials, theoretical tools such as the Hubbard model, and models derived from it in the limit of strong on-site repulsion, are commonly used in 2D (also in 3D) systems. These exhibit very interesting properties: in a model of bosons on the triangular lattice, doping away from commensurate fillings drives a transition from an insulator to a supersolid phase (with charge ordering and a finite superfluid density),[3] which is also found in a model of bosons on the checkerboard lattice;[4] on the same lattice, spinless fermions near 1/4 filling present interesting properties such as fractional charge excitations.[5,6]

In a more specific context, to describe the nonmagnetic resonating valence-bond phase of cuprate materials and the transition of this phase to the superconducting phase, the quantum dimer model (QDM) was developed in the late eighties,[7] mostly on two-dimensional lattices. This model displays different types of valence-bond crystals (with close analogies with their spin counterparts), among which the quite exotic *plaquette* phases, and, depending on the lattice (non-) bipartiteness, either a liquid phase with topological order (on the triangular lattice[8]) or a quantum critical point [Roksar-Kivelson (RK) point], both presenting deconfined excitations.[8] The QDM is also connected to the physics of pyrochlore systems, since strong Coulomb repulsion in the (extended) Hubbard model on the kagomé or on the checkerboard lattice, either for bosons or fermions at special fractional fillings, select low-energy configurations that can be mapped onto dimer or loop configurations.

The present study belongs to a series of works about the extended Hubbard model on the 2D pyrochlore (or checkerboard) lattice, at and slightly away from fractional

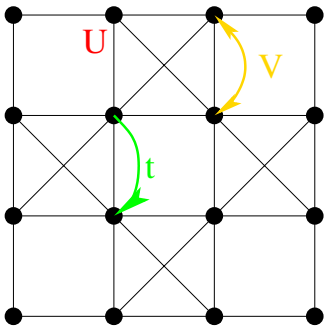

FIG. 1. (Color online) Schematic representation of the Hubbard model on the checkerboard lattice. In the limit $|t| \ll V \ll U$, this model becomes equivalent to that described by the Hamiltonian H_K [see Eq. (1.3)].

fillings.[5,9–11] Here we focus on the effective model of $S=1/2$ fermions at 1/8 filling (one particle for four sites) derived from the extended Hubbard model,

$$H = -t\sum_{\langle ij\rangle,\sigma} c^{\dagger}_{i,\sigma}c^{\dagger}_{j,\sigma} + U\sum_{i} n_{i\uparrow}n_{i\downarrow} + V\sum_{\langle i,j\rangle} n_i n_j, \qquad (1.1)$$

in the limit of large Coulomb repulsions U and V (with respect to the energy scale given by the particle hopping amplitude t). Let us briefly review our current understanding of the physics of the extended Hubbard model on the pyrochlore lattice at the special fractional fillings $n=k/4$ $(k=1,2,3)$(Refs. 9 and 10) and mention the important remaining issues. For spinful fermions at these fillings, in the limit where the on-site repulsion U is very large compared to the nearest-neighbor repulsion V and hopping t, a metal-to-insulator transition was found for increasing $|V/t|$ at the filling factor $n=1/4$ (similarly as in the corresponding hard-core bosonic model[11]), and the corresponding insulating phase (for $|t| \ll V \ll U$) exhibits plaquette correlations indicating an ordering very different from a simple charge-density wave. Whether the metal-to-insulator transition occurs immediately at infinitesimal V or at a finite value depends on the degree of the commensurability k. Indeed, the perfect nesting property of the noninteracting Fermi surface realized only for $k=2$ (and for a given sign of t) leads to an instability for arbitrarily small U and V.[12] In the limit of interest here (strong couplings), an effective model of $S=1/2$ fermions was derived in the same study, involving a two-particle hopping term (amplitude t_2) and an additional term (amplitude W) counting the number of singlet pairs on uncrossed plaquettes. Varying the ratio of the amplitudes of these terms, the system can be tuned from a charge-ordered *columnar* phase [the internal structure of columns being that of Heisenberg antiferromagnetic (AF) chains] in the limit $W \ll -|t_2|$ to a disordered RK point at $W=t_2$. Note that, in this formulation, the case $W=0$ is believed to provide the effective description of the insulating phase of the large-U, large-V Hubbard model on the checkerboard lattice mentioned above.

So far the case corresponding to filling $n=1/2$ is understood the best. A phase transition was clearly evidenced at finite (negative) W/t_2 between the charge-ordered phase and a resonating singlet-pair crystal (RSPC) using an analysis based on the symmetry-resolved low-energy spectrum and plaquette correlations in the ground state (GS). The system at $n=3/4$ was shown to exhibit also plaquette order by forming a (lattice rotationally invariant) resonating singlet-pair crystal, although with a quadrupling of the lattice unit cell (instead of a doubling for $n=1/2$) and a fourfold degenerate ground state. Concerning the $n=1/4$ case, the conclusions of the previous study were less clear. Although the evolution of plaquette correlations with W/t_2 also supports a transition from a charge-ordered to a RSPC, the analysis of low-energy eigenstates was less conclusive than in the $n=1/2$ and $n=3/4$ cases, primarily due to larger finite-size effects: in the previous study computations were done on a $N=32$ checkerboard cluster with periodic boundary conditions (PBC). Moreover for $n=1/4$, taking into account the possibility of new mixed phases (which are not charge-localized but break rotational symmetry) requires more caution in the analysis of the low-energy spectrum (and hence larger clusters). This leads us to consider a new scenario for the phase diagram of the model, which will be described in more detail hereafter.

B. Effective model

As outlined above, the effective model is derived from the extended Hubbard model for $S=1/2$ fermionic particles on the checkerboard lattice, in the limit of very large Coulomb repulsion (more precisely $|t| \ll V \ll U$). In this limit, at 1/8 filling ($n=1/4$), one can exclude configurations where the two neighboring sites are simultaneously occupied. In other words, each tetrahedra should contain exactly one particle (of either spin), an *ice rule*-type constraint, which still leaves an exponentially large number of states. As discussed in the literature, once the particles are viewed as dimers living on the bonds of the square lattice formed by the centers of crossed plaquettes, this constraint is equivalent to the *hard-core* dimer constraint on the square lattice. However, in contrast to the "usual" QDM on the square lattice, here each dimer carries a color index (associated to the spin of the electron it represents).

In this limit, a single particle that hops out of a low-energy configuration (*colored dimer* configuration) creates a defect centered on a tetrahedra with an energy cost V. This defect can however be annealed by the subsequent hopping of the second particle on the "defect tetrahedron." Such processes lead to an effective kinetic term, i.e., a correlated two-particle hopping, of amplitude $t_2=2t^2/V$. In terms of dimers, this term looks like the kinetic term of the RK model, but acts only on particles of opposite spin on the same uncrossed plaquette (i.e., dimers of opposite color on the same plaquette). The particles being fermionic, the expression of the kinetic term involves operators of creation (destruction) of singlets on uncrossed plaquettes, $c^{\dagger}_{i\uparrow}c^{\dagger}_{j\downarrow} - c^{\dagger}_{i\downarrow}c^{\dagger}_{j\uparrow}$ $(c_{i\uparrow}c_{j\downarrow} - c_{i\downarrow}c_{j\uparrow})$,

$$H_K = -t_2\sum_{\langle ijkl\rangle} [(c^{\dagger}_{i\uparrow}c^{\dagger}_{j\downarrow} - c^{\dagger}_{i\downarrow}c^{\dagger}_{j\uparrow}) \times (c_{k\uparrow}c_{l\downarrow} - c_{k\downarrow}c_{l\uparrow}) + \text{c.c.}], \qquad (1.2)$$

where the sum is on uncrossed plaquettes (going around a plaquette $\langle ijkl\rangle$, sites are in the order i, k, j, l). A unitary transformation, consisting in defining operators $b^{(\dagger)}_{i\downarrow} = -c^{(\dagger)}_{i\downarrow}$ on every other ascending and every other descending line of the checkerboard lattice oriented as in Fig. 1 (i.e., every other vertical line of vertical links and every other horizontal line of horizontal links of the associated square dimer lattice) and $b^{(\dagger)}_{i,\sigma} = c^{(\dagger)}_{i,\sigma}$ otherwise, allows that each two-particle hopping term to have the same amplitude $-t_2$ in terms of $b^{(\dagger)}_{i,\sigma}$ operators,

$$H_K = -t_2\sum_{\langle ijkl\rangle} [(b^{\dagger}_{i\uparrow}b^{\dagger}_{j\downarrow} + b^{\dagger}_{i\downarrow}b^{\dagger}_{j\uparrow}) \times (b_{k\uparrow}b_{l\downarrow} + b_{k\downarrow}b_{l\uparrow}) + \text{c.c.}]. \qquad (1.3)$$

Notice that this is valid only *in the insulating phases* at specific fractional fillings such as $n=1/4$, thanks to the ice rule-type constraint. In addition, it is possible to label the sites of the lattice in such a way that all exchange processes on the

empty squares do not involve any reordering of the fermions so that the $b_{i,\sigma}^{(\dagger)}$ operators can be considered as bosonic. In other words, our new formulation uses the bosonic representation of the spin singlets (we have checked the equivalence numerically on the 32-site cluster).

Following the initial suggestion of Ref. 9 and according to the discussion above, we also consider a term analogous to the potential term of the QDM, although here it is no longer diagonal in the basis of configurations,

$$H_W = W \sum_{\langle ijkl \rangle} [n_i n_j (1-n_k)(1-n_l)(1/2 - 2\mathbf{S}_i \cdot \mathbf{S}_j) + n_k n_l (1-n_i)(1-n_j)(1/2 - 2\mathbf{S}_k \cdot \mathbf{S}_l)]. \quad (1.4)$$

This terms "counts" the number of singlet pairs of next-nearest neighbors (*parallel dimers*) in all uncrossed plaquettes. The resulting Hamiltonian $H_W + H_K$ has a structure similar to that of the Roksar-Kivelson QDM, with both terms flipping dimers and terms counting the flippable pairs of dimers. H_W can also be interpreted as a four-site ring-exchange term on uncrossed plaquettes.[10] It also presents a RK point (here at $W=t_2$), while for $W/|t_2| \to -\infty$ an ordering in chains is favored; varying W/t_2 allows to make a continuous connection between both these limits and the case $W=0$, and to understand better the physics around this point.

C. Purpose of the study: phase diagram

Since t_2 and W are the only energy scales in this model (at zero temperature) we aim at determining the phase diagram as a function of the ratio W/t_2 (or W, if we set $t_2=1$). First, we notice that for $t_2=W$, the Hamiltonian has the same property as in the quantum dimer model at the RK point: it can be written as a sum of projectors (one per uncrossed plaquette). At this point (the RK point of the t_2-W model) the wave function with an equal amplitude on all configurations (in each sector of connected configurations) is annihilated by each projector, and thus is a ground state with zero energy. For $W \geq t_2$, again for similar reasons as in the QDM, configurations of minimal energy are those without any flippable pair of spins, and these configurations are (degenerate) ground states with zero energy. The center of interest of this study is the case where $W \leq t_2$, i.e., the region between the RK point and the $W=-\infty$ point, where the ground state is composed of decoupled Heisenberg chains (its energy is the sum of the energy of these chains with an AF coupling $J=2|W|$ and a *charge* term $L_{\text{tot}}W/2$ where L_{tot} is the cumulative length of the chains). Instead of considering W and t_2, one can define a reduced parameter $\theta=\arctan(W/t_2)$ varying continuously between the decoupled Heisenberg chains ($\theta=-\pi/2$) and the RK point ($\theta=\pi/4$).

Between these points, the different phases one can expect are (i) a *columnar* phase, ordered in chains, with rotational symmetry breaking, translational symmetry breaking in one direction (perpendicular to the chains) and thus a fourfold degeneracy of the corresponding ground state; this phase is encountered for $\theta=-\pi/2$, and could *a priori* extend over a finite range of θ in the vicinity of that point. Note that the term *columnar* is used although this phase differs from the columnar phase of the QDM on the square lattice, due to the additional spin degrees of freedom; (ii) a RSPC or *plaquette* phase, with the full rotational symmetry of the lattice but a breaking of translational symmetry in both directions and a fourfold degeneracy of the GS; (iii) mixed phases, with rotational and translational (in both directions) symmetry breaking (and a eightfold degenerate GS), corresponding to a dimerization of the Heisenberg chains. *A priori* two types of mixed phases appear naturally depending whether neighboring chains dimerize in phase, or in antiphase. Note that these phases are a natural extension of the one recently discovered in the context of the RK QDM.[13] We shall refer to them as *mixed columnar-plaquette crystals* (MCPC).

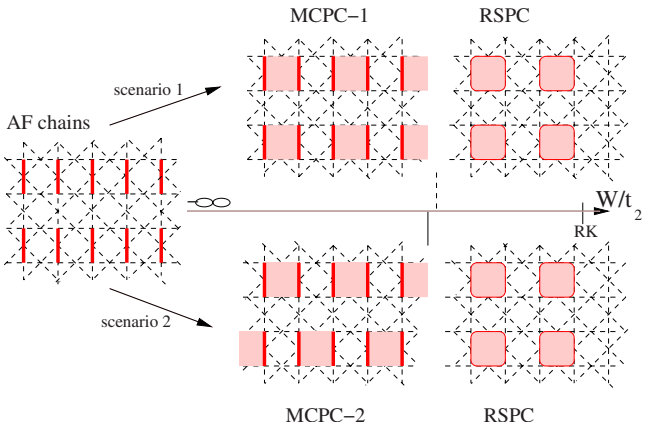

FIG. 2. (Color online) Possible scenarios for phase diagrams at $n=1/4$ as a function of the ratio of parameters W/t_2, depending whether an infinitesimal t_2 coupling dimerizes AF chains from a columnar order into a *mixed columnar-plaquette crystal* of type 1 (MCPC-1, up) or 2 (MCPC-2, down). The transitions indicated between either of these phases and a RSPC should be presumably of first order in the first case and second order in the second case, but one cannot exclude that the MCPC phase extends all the way to the *RK* point.

Knowing that $\theta=-\pi/2$ corresponds to a columnar phase, we refer in phase or in antiphase dimerization as MCPC-1 and MCPC-2, respectively, as shown schematically in Fig. 2. These phases have distinct symmetries and the corresponding ground states are characterized by different sets of (four or eight) quantum numbers, which we define using the following conventions: the x and y axes of the lattice are parallel to the links of the square lattice (on which the *dimers* live), and the unit length corresponds to one link of this square lattice. To define point-group symmetries (those of the C_{4v} point group—or C_{2v} or C_v for certain wave vectors) we set the center O of the lattice at the center of an uncrossed plaquette. The quantum numbers of the degenerate GS of the various phases are listed in Table I.

Given the symmetries of the candidate phases, one can make a guess about the nature of phase transitions in the model, for both scenarios described in Fig. 2. In the case of a MCPC-2 phase for $|t_2| \ll -W$, giving way to a RSPC close to the RK point, the transition between those should be of first order, since the symmetry groups of one phase is not included in that of the other. By contrast, since the MCPC-1 phase distinguishes itself from the RSPC by the breaking of

TABLE I. Quantum numbers of the degenerate GS (in the thermodynamic limit) associated with the various phases expected in the t_2-W model at $n=1/4$ on the checkerboard lattice (for $W \leq t_2$). The X sign indicates that a wave function with the corresponding quantum number belongs to the degenerate GS manifold for the corresponding phase (0 otherwise). Irreducible representations labeled with $'$ are respective to subgroups C_{2v} $(A'1)$ and C_v (A',B') of the point group C_{4v} when the wave vector considered is noninvariant under C_{4v}.

Phase →	MCPC-1	MCPC-2	RSPC	Columnar
$[A1,q=(0,0)]$	X	X	X	X
$[B1,q=(0,0)]$	X	X	0	X
$[A1,q=(\pi,\pi)]$	X	0	X	0
$[A'1,q=(\pi,0)](1)$	X	X	X	X
$[B1,q=(\pi,\pi)]$	X	0	0	0
$[A'1,q=(\pi,0)](2)$	X	0	0	0
$[B',q=(\pi/2,\pi)]$	0	X	0	0

one of its symmetries (invariance by a $\pi/2$ rotation), the transition between those could be of second order.

D. Methods

In the present work, we first discuss the regime near $W/t_2=-\infty$ perturbatively (Sec. II). Next, we implement a simple variational approach (discussed further in Sec. III) adapted to describing the various candidate phases; in a second step, we shall use Lanczos exact diagonalization techniques to study the t_2-W model on clusters with periodic boundary conditions in both directions. The sizes of the clusters we consider in numerics are $N=32,72$ ($\pi/4$-tilted checkerboard clusters corresponding to untilted square clusters of lengths $L=4,6$), $N=48$ [$\pi/4$-tilted checkerboard cluster corresponding to an untilted rectangular cluster of dimensions $(L_x,L_y)=(4,6)$], and $N=64$ (untilted checkerboard cluster corresponding to a $\pi/4$-tilted square lattice of length $L=4\sqrt{2}$). Except for $N=72$, the cluster periodicity is compatible with all wave vectors $\mathbf{q}$ mentioned in the table above [for the $N=72$ cluster, the wave vector $\mathbf{q}=(\pi/2,\pi)$ and those equivalent to it up to point-group symmetries are unaccessible].

Note that we restrict ourselves to the sector $S_z=0$ (which includes all total spin sectors)—for convenience. In addition, we consider only configurations for which the z components of the total spin on each row (of vertical bonds) and each column (of horizontal bonds) of the square lattice (which are conserved quantities in the present model) are zero. This condition is satisfied by the ground states corresponding to any of the expected phases, and allows us to reduce the number of colorings of any dimer (=charge) configuration (hence the total size of the Hilbert space). By using the character of spin inversion, all point-group symmetries and translations (in fact, due to the numerical technique for encoding configurations, we use translations not interchanging the sublattices of the dimer lattice, hence $N/4$ translations instead of $N/2$) the number of representatives for $N=64$ and $N=72$ clusters are close to 4.5×10^4 and 1.9×10^5, respectively.[14]

A powerful tool to determine the phase diagram is the analysis of the lowest energy levels in symmetry sectors associated to each of the quantum numbers mentioned (and with a character 1 for the spin inversion $S_i^z \to -S_i^z$). For the various phases one expects a degeneracy between the quantum numbers marked by X in Table I, in the thermodynamic limit ($N\to\infty$). On finite clusters, this degeneracy is lifted and the lowest state is always found for $[A1,\mathbf{q}=(0,0)]$—hence we look at the lowest excited states. Ideally, an unambiguous signal of spontaneous symmetry breaking is provided by the collapse of the corresponding excitation energies $\Delta E=E_i-E_0[A1,(0,0)]$ with increasing N. However, the low-energy spectrum on a large enough cluster (e.g., $N=64$) gives enough information for a first analysis.

II. PERTURBATIVE APPROACH FROM $W=-\infty$: COUPLING OF HEISENBERG CHAINS

Adding the potential term W to the Hamiltonian has several benefits, among them the existence of two particularly simple special points, namely the RK point, and the point at $W=-\infty$. For the bosonic model, the latter yields the simple columnar configurations as ground states. However, $W=-\infty$ does not always present such a simple setting. For the triangular RK model, there are two families of ground states, each comprising a number of members exponential in the linear system size, the degeneracy between which is not lifted until perturbations to leading nontrivial order in t_2/W are taken into account.[8]

The situation for our model is different still. *At* $W=-\infty$, the ground state is obtained by maximizing the number of plaquettes with a pair of dimers in a singlet configuration. This leads to formation of a state breaking rotational and translational symmetries—just like the columnar state—but in which the spin correlations along the columns are critical. Indeed, $W=-\infty$ corresponds to decoupled Heisenberg chains.

The question appropriate to the setting of small $|t_2/W|$ is thus what is the most relevant perturbation induced by the kinetic term. This question has been addressed in—formally related—contexts by Starykh and co-workers[15] and Essler and co-workers.[16] We closely follow the approach of the latter. Their observation that in the Heisenberg chain not only the staggered spin but also the staggered energy correlations are critical—both decay as $1/r$—is central: the chains are close to not only Neel but also to dimer ordering.

For our model, the coupling of the staggered dimerization between neighboring chains is symmetry allowed, and hence will generically appear as a perturbation is added. Indeed, it is easy to see how this happens in our model. For finite $|t_2/W|$, flipping the dimers in two neighboring plaquettes in adjacent rows yields an energy gain of $O(W)$ for the plaquette marked by a cross in Fig. 3, whereas there is no such gain for the two plaquettes marked by circles. The coupling between the chains is thus generated at $O(|t_2/W|^4)$, as each plaquette needs to be flipped out of the chain and back.

As analyzed in Ref. 15, this coupling is relevant and it will immediately lead to an in-phase dimerization of adjacent chains. In our above classification, this corresponds to a

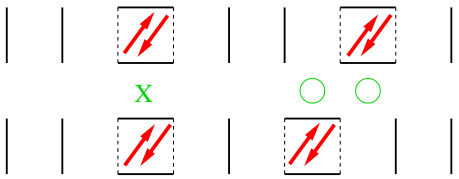

FIG. 3. (Color online) Origin of dimerization in the limit of large negative W (singlets flipped by H_K are represented by an up-down spin pair): the plaquette marked by a cross gains an energy $W/2$, while there is no such gain on plaquettes marked by circles.

MCPC-1 phase, which is thus present in the limit $W/t_2 \to -\infty$.

Before we move on to variational (Sec. III) and numerical (Secs. IV and V) investigations of the effective t_2-W model on the checkerboard lattice, let us make some further remarks on the regime where $W/t_2 \ll -1$. This will serve as a warm-up exercise for identifying ground states by quantum numbers. Let us consider a pair of Heisenberg chains of length L (with periodic boundary conditions, the chain axis being x), of spins-1/2 $S_{i,1}$ and $S_{i,2}$. The Hamiltonian

$$H = J\sum_{i,\alpha} \mathbf{S}_{i,\alpha}\cdot\mathbf{S}_{i+1,\alpha} + K\sum_{i} (\mathbf{S}_{i,1}\cdot\mathbf{S}_{i+1,1})(\mathbf{S}_{i,2}\cdot\mathbf{S}_{i+1,2})$$

captures then coupling described above, although the true effective coupling is more complicated; in particular, it includes similar four-spin terms along the chain favoring the same dimerization pattern.

At $K=0$, the ground state is the product of ground states of the Heisenberg model on each chain, and has a symmetry $(A,k_x=0)$– A (B) labeling even (odd) states with respect to the chain interchange (Fig. 4). The first excited state in the $S=0$ sector corresponds to a 2-triplet excitation on one chain (the other chain remaining in the GS). It is doubly degenerate, the quantum numbers of both states being $(A,k_x=\pi)$ and $(B,k_x=\pi)$. This state has (similarly to 1-triplet excitations) an excitation energy proportional to $1/L$, thus collapsing to the ground state in the thermodynamic limit.

When a weak interchain coupling K is added, the degeneracy of this first excited state is lifted, with a splitting proportional to K/J, as shown in Fig. 5. Since each of these states has the symmetry of a dimerized state, with dimerization either in phase [state (A,π)] or in antiphase [state (B,π)], the sign of this splitting is therefore associated with the type of dimerization susceptible to spontaneously appear in the system: for $K/J \geq 0$, the (B,π) state has a lower energy than the (A,π) state and the system tends to dimerize in antiphase; this is the opposite case for $K/J \leq 0$.

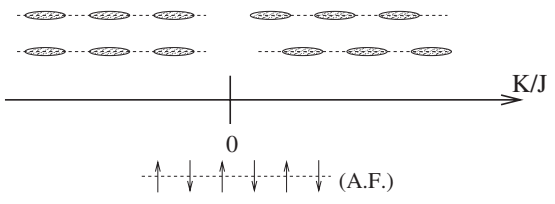

FIG. 4. Types of dimerization occurring in two Heisenberg chains coupled by a four-spin coupling: in-phase dimerization ($K \leq 0$) or antiphase dimerization ($K \geq 0$).

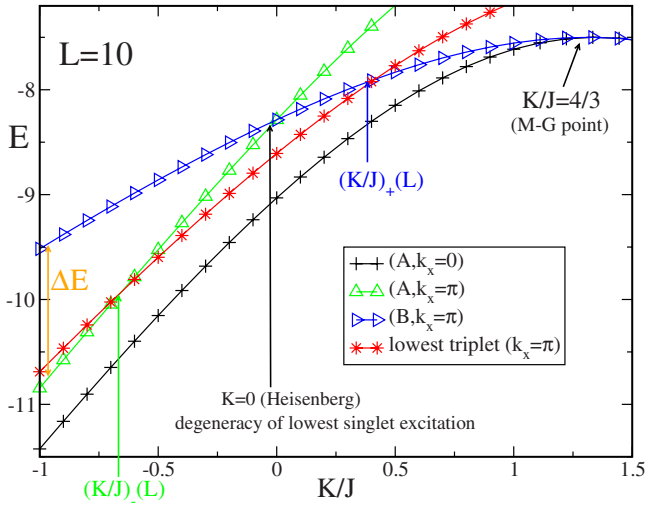

FIG. 5. (Color online) Energies of the ground state and first excited states of two periodic Heisenberg chains of $L=10$ spins 1/2 (Heisenberg coupling J) coupled with a four-spin interchain coupling K. $(K/J)_c$ indicates the crossing between the lowest triplet and the $(A,k_x=\pi)$ singlet. Notice also the degeneracy of $(B,k_x=\pi)$ and $(A,k_x=0)$ states at the Majumdar-Ghosh point $K/J=4/3$.

Let us examine now the finite-size scaling of these excitations in the presence of the four-spin coupling. The excitation energy of the lowest excited singlet state [(A,π) for $K \leq 0$ and (B,π) for $K \geq 0$] vanishes in the thermodynamic limit (the convergence is as $1/L$ for $K/J \ll 1$), while the excitation energy to the lowest triplet converges to a finite value (spin gap) (see right plot in Fig. 6). Consequently, while on a small enough system the triplet excitation has lower energy than the lowest singlet, these levels cross as a function of system size (at fixed K/J). This is illustrated (in

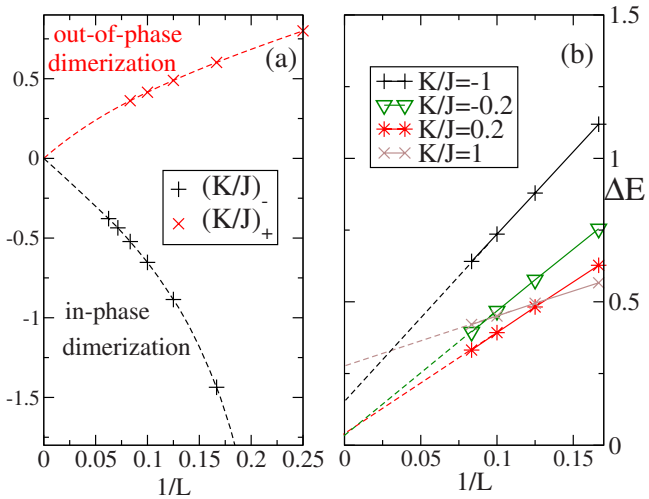

FIG. 6. (a) (Color online) Position of the energy crossings between the lowest triplet and lowest (A,π) [$(K/J)_-$] and (B,π) [$(K/J)_+$] singlet states as a function of $1/L$ (L even up to 16); (b) excitation energy ΔE of the lowest triplet for different values of K/J versus $1/L$. Dashed lines are only a guide for the eyes.

a slightly different way) by the left plot in Fig. 6, showing the positions of crossings $(K/J)_{+/-}(L)$ between the lowest triplet and either the lowest (A,π) or (B,π) singlet, as a function of system size. One can see that these values converge to zero as $L\to\infty$. (Rigorously, one cannot be fully conclusive with the present data set but a vanishing value as $L\to\infty$ is expected from the reasoning above. Moreover we checked that expressions of the type $C/L+C'/L^2$ fit the data of $(K/J)_{+/-}$ better than any expression of the type $C+C'/L^{\alpha}$.) Therefore the lowest singlet excitation, of symmetry either (A,π) or (B,π) depending of the sign of K, collapses onto the GS in the thermodynamic limit while a spin gap survives above. This is the well-known scenario of a spontaneous dimerization, which is precisely the type of scenario one expects in our two-dimensional effective model in the limit of weakly coupled chains (of colored dimers). Here, it is important to note that there are distinct reasons for the vanishing gaps. Even for $W=-\infty$, there will be finite-size gaps of $O(|W|)$, which vanishes algebraically due to the criticality of the chains, while the other gap, parametrically small in $|t_2/W|$, collapses due to the presence of symmetry breaking.

III. VARIATIONAL APPROACH DESCRIBING THE CANDIDATE PHASES

A. Principle and trial wave functions

Before analyzing the exact ground state and lowest excitations on finite systems, we estimate the energies of trial wave functions associated with the different candidate (RSPC, MCPC-1, and MCPC-2) phases in the range of parameters of interest $(-\pi/2\leq\theta\leq\pi/4)$. A comparison between their variational energies provides information on their relative stability. The trial wave functions we consider are built as the tensor product on all equivalent plaquettes of an identical wave function $|\psi_p\rangle$ defined on a single uncrossed plaquette p, with a resonating singlet delocalized on the four sites of the plaquette.

On this plaquette, $|\psi_p\rangle$ is expanded over the four $S_z=0$ configurations with two particles on the plaquette (and respecting the *dimer* constraint). If the four sites of the plaquette are labeled from 1 to 4 clockwise around the plaquette (starting from e.g., the site on the upper left side) these four configurations are as follows: $|u\rangle=|\uparrow_1 0_2\downarrow_3 0_4\rangle$ (0 denoting an empty site); $|d\rangle=|\downarrow_1 0_2\uparrow_3 0_4\rangle$; $|r\rangle=|0_1\uparrow_2 0_3\downarrow_4\rangle$ and $|l\rangle=|0_1\downarrow_2 0_3\uparrow_4\rangle$. $\psi_p(\phi)$ is a linear combination of the two singlet states $(|u\rangle+|d\rangle)/\sqrt{2}$ and $(|r\rangle+|l\rangle)/\sqrt{2}$ (the plus sign results from the unitary transformation mentioned in Sec. I B):

$$|\psi_p\rangle(\phi)=\cos(\phi)\frac{|u\rangle+|d\rangle}{\sqrt{2}}+\sin(\phi)\frac{|r\rangle+|l\rangle}{\sqrt{2}}.$$

The parameter ϕ can be restricted to values between 0 and $\pi/4$, thus describing mixed phases obtained by dimerization of horizontally oriented Heisenberg chains. The global wave function on a N-site cluster $|\Psi_0(\phi)\rangle=\otimes_{i=1}^{N/8}|\psi_{p_i}(\phi)\rangle$ depends on the angle ϕ and the set of $N/8$ chosen plaquettes p_i, i.e., the type of dimerization described: either in phase (MCPC-1) or in antiphase (MCPC-2). In the first case the RSPC corresponds to an angle $\phi=\pi/4$. The wave function $|\Psi_0\rangle$ need not be symmetrized with respect to space group symmetries, in order to compute the expectation values of H_K and H_W in the thermodynamic limit: indeed, for two symmetry-related and distinct vectors $|\Psi_0\rangle$ and $|\Psi_0'\rangle$, quantities such as $\langle\Psi_0'|H_{K/W}|\Psi_0\rangle$ give a relative contribution $O(1/N)$.

B. Trial function for MCPC-1 and RSPC phases

In order to describe the MCPC-1 phase and its stability with respect to the RSPC, the trial wave function $|\Psi_0^1\rangle(\phi)$ is used to compute expectation values of H_K and H_W. The only terms of H_K contributing to $\langle\Psi_0^1|H_K|\Psi_0^1\rangle$ are plaquette flips on occupied plaquettes, exchanging u/d configurations and r/l ones. The average kinetic energy (per particle) is then

$$H_{K,1}(\phi)=4/N\langle\Psi_0^1|H_K|\Psi_0^1\rangle=-2t_2\sin(\phi)\cos(\phi). \quad (2.1)$$

For the nondiagonal part of H_W (with $S_i^+S_j^-$ terms), again only terms for which both sites are in an occupied plaquette contribute. But concerning the diagonal part of H_W, terms $1/2-2S_i^zS_j^z$ with i, j on a void plaquette between two occupied plaquettes also contribute, proportionally to either $\cos(\phi)^4$ or $\sin(\phi)^4$ depending on the position of this void plaquette. The expectation value of H_W (still per particle) is

$$H_{W,1}(\phi)=4/N\langle\Psi_0^1|H_W|\Psi_0^1\rangle=W[1+\sin(\phi)^4/4+\cos(\phi)^4/4]. \quad (2.2)$$

The minimization of $\langle H_K(\phi)\rangle+\langle H_W(\phi)\rangle$ with respect to ϕ can lead to two distinct cases. For $W/t_2\leq-4$ a nontrivial value ϕ_1 of ϕ minimizing the expectation value of $H=H_K+H_W$ is found, corresponding to a MCPC-1 state breaking the $\pi/2$-rotational symmetry. ϕ_1 is solution of $W/t_2=-4/\sin(\phi_1)$, and the corresponding average energy is

$$E_1(\phi_1)=2\frac{t_2^2}{W}+5W/4.$$

For $W/t_2\geq-4$ the minimization gives $\phi_1=\pi/4$, which means that the rotationally invariant RSPC is the most favorable state in this approach. The average energy of the RSPC is estimated as

$$E_1(\pi/4)=-t_2+9W/8.$$

The energies $E_1(\pi/4)$ and [for $\theta\leq\arctan(-4)$] $E_1(\phi_1)$ are shown as a function of the parameter θ in Fig. 7. Notice that for $\theta\leq\arctan(-4)$, $H_1(\pi/4)$ corresponds to a local maximum of the function $H_1(\phi)$ and is shown only for comparison to the (physically relevant) MCPC-1 variational energy $E_1(\phi_1)$.

These results give also an indication of the nature of the MCPC-1/RSPC transition: the expansion of the variational energy functional $H_{K,1}+H_{W,1}(\phi)$ in powers of $x=\phi-\pi/4$, for W/t_2 close to -4, is

$$H_1(\phi)=H_1(\pi/4)+2(t_2+W/4)x^2+(-19W/24-2t_2/3)x^4.$$

The sign of the coefficient of the x^2 term changes for $W=-4t_2$ while that of the x^4 term remains positive around that point: in the frame of Landau's theory of phase transitions, this is characteristic of a second-order transition with x as an order parameter, which varies continuously around

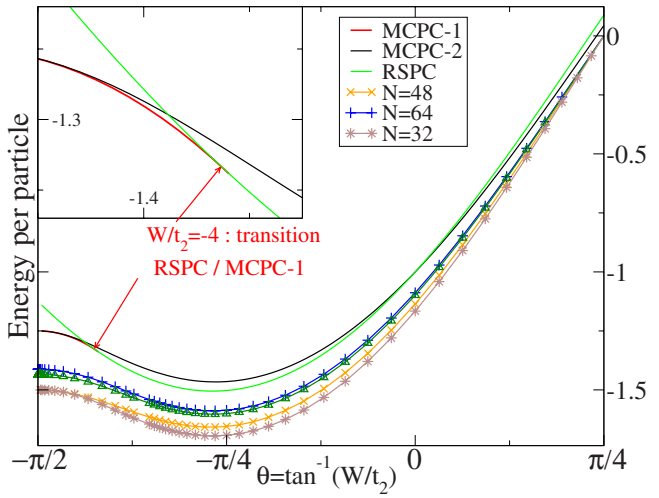

FIG. 7. (Color online) Energies (per particle and in units of $\sqrt{t_2^2+W^2}$) of variational ground states describing the MCPC-1 [$\theta \leq \arctan(-4)$], RSPC and MCPC-2 phases as a function of θ. Exact ground-state energies for $N=32$, 48, 64, and 72 clusters are shown for comparison.

the MCPC-1/RSPC transition and vanishes in the $\pi/2$-rotationally invariant phase.

C. Trial function for the MCPC-2 phase

In this case, the trial wave function $|\Psi_0^2\rangle$ is still parametrized by an angle ϕ between 0 and $\pi/4$ and differs only from the wave function describing the MCPC-1 phase by the position of the occupied plaquettes. The angle $\pi/4$ corresponds here to a rotationally noninvariant pattern of rotationally invariant occupied plaquettes (which differs from the RSPC). Again, the structure of the trial state implies that the contribution to the expectation values of H_K and the nondiagonal part of H_W comes only from terms acting independently on occupied plaquettes. But here the diagonal part of H_W acts differently on the wave function than in the previous case: it gives a nonzero expectation value only on the void plaquettes situated between 2 occupied plaquettes to the right and left (see Fig. 2). The corresponding term in $\langle H_W \rangle$ is thus proportional to the probability $\cos(\phi)^4$ for particles of both plaquettes to be in $|r\rangle$ or $|l\rangle$ states. Eventually the expectation value of H as a function of ϕ reads

$$H_2(\phi) = 4/N\langle\Psi_0^2|H_W + H_K|\Psi_0^2\rangle = W[1+\cos(\phi)^4/4] - 2t_2\cos(\phi)\sin(\phi) \quad (2.3)$$

and is minimized, either for $\phi_2=\pi/4$ when $W\geq 0$, or when $W\leq 0$ for ϕ_2 solution of

$$W/t_2 = -4\frac{1+\tan(\phi_2)^2}{\tan(2\phi_2)}.$$

The angle ϕ_2 (for $W\leq 0$), and consequently the corresponding expectation value $E_2(\phi_2)$ of H, has no simple expression as a function of W/t_2 or θ; a numerical resolution proves that

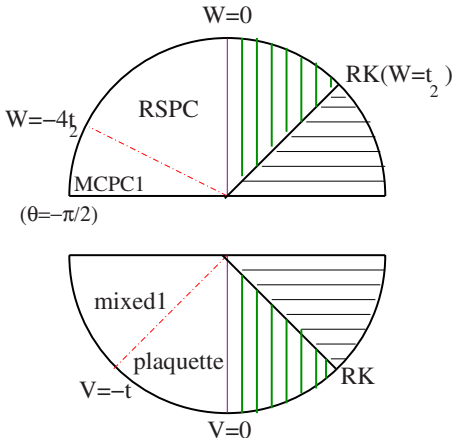

FIG. 8. (Color online) Variational phase diagrams for the model of fermions (up) or bosons (down, with notations of Ref. 13). The point of transition between a $\pi/2$-rotational invariant phase and a phase breaking that symmetry is predicted at $W=-t_2$ (for fermions) and $V=-t$ (for bosons). For $0\leq W\leq t_2$ (resp. $0\leq V\leq t$) the MCPC-2 or mixed-2 phase is the most competitive of our crystalline trial wave functions, but it in turn loses out to the simple RK wave function; see III E (green vertical lines).

for $W\leq 0$ it is greater than $H_1(\phi_1)$ found with the wave function $|\Psi_0^1\rangle$ (see Fig. 7)—this is not a surprise since the $(W/4)\sin(\phi)^4$ term present in Eq. (2.2) is absent in Eq. (2.3). In other words, this approach indicates that the MCPC-1 or RSPC phase is stabilized with respect to the MCPC-2 phase by interactions on some plaquettes, as soon as they are attractive ($W<0$).

For $W\geq 0$ the variational ground state $|\Psi_0^2\rangle$ corresponding to an angle $\phi_2=\pi/4$ has an energy $17W/16-t_2$ lower than that of the RSPC found before. Hence this can be considered as the variational ground state in this approach, predicting a domain of stability $-4t_2<W<0$ for the MCPC-1 phase (see Fig. 8)—but one has to take into account the limitations of this approach, discussed in III E.

D. Comparison to the bosonic case

In this paragraph we apply the previous variational method to the bosonic case, i.e., to the QDM of Roksar and Kivelson on the square lattice, to have a comparison between the variational and exact phase diagrams. In this case, a variational wave function $|\Psi\rangle(\phi)$ describing the plaquette phase and the mixed phase (both described in Ref. 13, i.e., the bosonic analog of the MCPC-1 phase ; similarly a *mixed 2* phase can be defined as the bosonic analog of the MCPC-2 phase) is defined, as previously, as a product of local wave functions on plaquettes occupied in a plaquette pattern:

$$|\Psi_p\rangle = \cos(\phi)|v\rangle + \sin(\phi)|h\rangle$$

($|v\rangle$ and $|h\rangle$ correspond to either 2 vertical or 2 horizontal dimers on the given plaquette). The energy per particle of the state $|\Psi\rangle(\phi)$ is here ($-t$ and V being the amplitudes of the kinetic and potential terms in the QDM, defined as in Ref. 13):

$$H_1(\phi) = -2t\,\sin(\phi)\cos(\phi) + V[1+\cos^4(\phi)+\sin^4(\phi)].$$

For $V \geq -t$ this is minimized for $\phi = \pi/4$ which corresponds to a plaquette state, while for $V \leq -t$ the angle ϕ_1 is such that $V/t = -1/\sin(2\phi_1)$. The corresponding energy per particle is

$$E_1(\phi_1) = \frac{t^2}{4V} + V \quad (V/t \leq -1),$$

$$E_1(\pi/4) = 3V/4 - t/2 \quad (V/t \geq -1).$$

As in the fermionic case, one can define a variational wave function parametrized by an angle ϕ' and corresponding to the *mixed 2* phase, and show that, after minimization with respect to ϕ' it has a lower energy than $E_1(\pi/4)$; but again, in that case the variational method is not adapted to the situation close to the RK point.

Consequently, the variational approach for bosons on the checkerboard at $n=1/4$ predicts the existence of a *mixed* phase for $V \leq -t$ and a transition (second order again) to a plaquette phase at $V=-t$. In this approach the plaquette phase extends from that point up to $V=0$, while the ground-state energy in the domain $0 \leq V \leq t$ is better approximated with a variational wave function of type *mixed-2*—this is essentially due to the inadequacy of this method close to the RK point. The variational phase diagrams for both the fermionic and the bosonic model (both for an average occupation number $n=1/4$) are shown in Fig. 8.

The larger extent of the RSPC phase in the fermionic model than of the plaquette phase in the bosonic can be attributed to the fact that, in the first case, a singlet resonating on a plaquette in a RSPC phase is less coupled to neighboring occupied plaquettes: the process coupling neighboring plaquettes is subject to the constraint that interacting particles have opposite spin, this constraint being absent in the bosonic case. Consequently, for fermions the RSPC phase is more stable and the transition to a MCPC phase with longer range correlations occurs for a larger (negative) value of W.

E. Reliability of the variational approach—comparison to exact ground-state energies

Let us now comment briefly on the reliability of this variational approach to give a qualitative, or even quantitative, estimation of the phase diagram. For this, we have compared the variational ground-state energies $H_1(\phi_1)$ and $H_2(\phi_2)$ to the exact ground-state energies obtained on periodic clusters of size $N=32$, 48, 64, and 72 (see Fig. 7). Since the orientation and geometrical shape of these clusters differ from each other, one cannot do an accurate finite-size scaling of the exact ground-state energy that would allow for a precise comparison between exact and variational energies in the thermodynamic limit. However, it appears clearly that finite-size effects on the exact energies (per particle) decrease with N, which suggests that for a wide range of θ (between $-3\pi/8$ and 0) the exact and variational ground-state energies differ from about 5% or less, and their variations with θ are very similar.[17] The discrepancy between exact and variational results is larger (i) when θ gets close to $\pi/4$: at the RK point, the ground-state energy on any cluster considered is zero while the variational energy per spin is $t_2/16$ and corresponds to a MCPC-2 phase unexpected here: the failure of the variational approach close to the RK point originates in the inadequacy of the variational wave function when the exact ground state is much more disordered (which holds also in the bosonic case); there, the RK wave function is a better trial wave function, with an energy per particle $E_{\mathrm{RK}}=W-t_2$ [$(V-t)/2$ in the bosonic case].[18] This RK trial wave function has an energy lower than $|\Psi_0^2\rangle$ for either $W/t_2 \geq 0$ or $V/t \geq 0$ (see Fig. 8), defining a domain of stability of a RK *phase*, which has to be interpreted more appropriately as a domain where the variational approach fails; (ii) in the t_2-W model when θ is close to $-\pi/2$, the failure of this variational approach is expected since the exact ground state consists of Heisenberg chains (weakly dimerized for finite t_2), with spin-spin correlations along chains slowly decaying and the trial wave functions describing isolated resonating plaquettes are no more valid there. For that reason, the position of the MCPC-1/RSPC transition, predicted in this approach at $W/t_2=-4$ [hence $\theta=-1.326(1)$ relatively close to $-\pi/2$] can differ appreciably from the real position of this transition. To determine the latter, one has to treat the model exactly, taking all allowed configurations into account (and not only those characteristic of the *plaquette* ordering) by methods such as exact diagonalization.

IV. ANALYSIS OF THE LOW-ENERGY SPECTRUM AND IDENTIFICATION OF PHASES

In the limit $t_2 \ll |W|$ of the t_2-W model, where the variational approach of Sec. III is least reliable, the kinetic term H_K can be described as a perturbation, while the unperturbed Hamiltonian H_W has for ground state a product of Heisenberg chains. The effect of H_K can be described by an effective coupling $K_{\mathrm{eff}}\, W|t_2/W|^4$, associated with processes of order 4 out of the Heisenberg ground state, where two singlets belonging to two neighboring chains and opposite to each other are flipped and then flipped back; the interaction resulting from this process is attractive due to the H_W term on the interchain plaquette(s), making this process the most important one in perturbation in t_2/W (among those having an influence on the type of dimerization). Although we did not determine analytically the sign of this effective coupling for $0 < t_2 \ll |W|$, by analyzing the energy splitting of the analogs on the checkerboard of the (A,π) and (B,π) excitations (of the two-chain $J-K$ model) we determine the sign of K_{eff}, i.e., the type of dimerization occurring in the system.

A. Weak-coupling regime: low-energy spectrum and quantum numbers

Let us consider first the $t_2=0$ limit: here the low-energy spectrum has a simple structure; i.e., lowest states are composed of lowest states of Heisenberg chain of the corresponding length (three chains of $L=6$ for the $N=72$ cluster, two chains of $L=4.k$ for the $N=32.k$ cluster ($k=1,2$). The ground state is found in sectors $[A1,(0,0)]$, $[B1,(0,0)]$, $[A'1,(\pi,0)]$, and $[A'1,(0,\pi)]$ (the fourfold degeneracy ac-

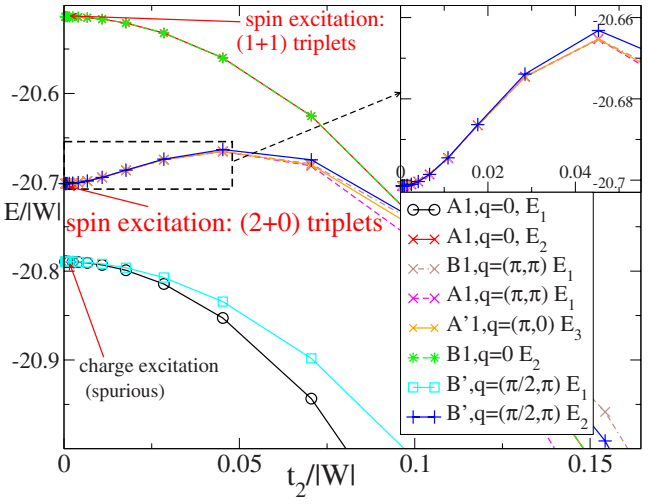

FIG. 9. (Color online) Energies of lowest excited states (in the $S=0$ sector) of symmetries $A1/B1,\mathbf{q}=(0,0)/(\pi,\pi)$, $[A'1,(\pi,0)]$, $[B',(\pi/2,\pi)]$, at $t_2 \ll |W|$, for a cluster of $N=64$ sites. Inset: splitting between a 2-triplet $[B',(\pi/2,\pi)]$ state (plus symbol) and other 2-triplet states (X symbols).

counts for the four ways of regularly accommodating two Heisenberg chains on the checkerboard cluster). At $t_2=0$, and by extension in the weak-coupling regime $|t_2/W| \ll 1$, the first excited states are, either on the cluster $N=64$ (see Fig. 9) or $N=72$: (i) a state in the $S=1$ sector (degenerate between various quantum numbers) corresponding to a 1-triplet excitation on one chain and the Heisenberg ground state of the other(s) chain(s); (ii) a state in the sector $S=0$, with all quantum numbers listed in Table I, corresponding to a charge excitation breaking a Heisenberg chain into an isolated singlet and an open $(L-2)$ chain; (iii) a state in the sector $S=0$ corresponding to 2-triplet excitation on the same Heisenberg chain, the other chains being in their ground states. On the $N=64$ cluster this state is found with the quantum numbers $[A1,(\pi,\pi)]$, $[B1,(\pi,\pi)]$, $[A'1,(\pi,0)]$, $[B',(\pi/2,\pi)]$ (and those related by symmetry); (iv) slightly above the latter, a state in the sector $S=0$ corresponding to two 1-triplet excitations on distinct chains.

Although the lowest excitation in the $S=0$ sector is, on clusters considered, the charge excitation, as far as these states can be labeled as *charge* and *2-triplet* excitations we rather focus on 2-triplet excitations [states (iii) and (iv)], since their excitation energy is a finite-size effect, being proportional to $|W|/L$ which vanishes in the thermodynamic limit, while state (ii) has an excitation energy of order $|W|$ even for $L \to \infty$. Among 2-triplet excitations, state (iii) (2 triplets on the same chain) is of greater interest: not only does it have a slightly lower energy than state (iv), but a reasoning based on the model situation of two Heisenberg chains coupled by a four-spin coupling term (see Sec. II) shows that this state gives information about the type of dimerization favored by the interchain coupling (or t_2 here).

To analyze the influence of a weak kinetic coupling $t_2 \ll |W|$ on the system and determine, in light of previously discussed features of the $J-K$ model of coupled Heisenberg chains, we focus on states with 2-triplet excitations on the same chain. The states corresponding to this excitation with different quantum numbers split when t_2 increases; at lowest order in $t_2/|W|$ the splitting occurs between the state in $[B',(\pi/2,\pi)]$ [2D analog of the (B,π) 2-triplet state in two coupled Heisenberg chains, hereafter *B state*] and states with other quantum numbers [analogs of the (A,π) 2-triplet excitation for two coupled Heisenberg chains; hereafter *A states*]. In this splitting the *B state* (associated with a dimerization in antiphase) has higher energy than the *A states* (associated with a dimerization in phase); moreover, we have checked that the energy difference between the *B state* and the *A states* scales as $W(t_2/W)^4$, as expected from the previously discussed comparison with the $J-K$ model of two Heisenberg chains (where the corresponding splitting occurs linearly in K/J). Hence we conclude that on the checkerboard, for small but finite $t_2/|W|$ the Heisenberg chains dimerize in phase and form a MCPC-1 phase, which is consistent with results of Sec. III.

While in the limit of small t_2/W the physics of the model is quasi-1D, making finite-size effects very important on the checkerboard clusters analyzed (especially at $t_2=0$, Heisenberg chains being critical), for larger couplings these finite-size effects become less relevant, as soon as the clusters can accommodate the various ordered phases. Hence in the latter case and with the cluster sizes available, it is reasonable to analyze the t_2-W model nonperturbatively, and without making reference to an effective model (such as that of coupled Heisenberg chains).

B. Nonperturbative analysis for intermediate W/t_2: MCPC-1 or RSPC phase?

Away from the $t_2 \ll |W|$ limit, one cannot simply identify each of the first excitations as *2-triplet* or *charge* excitations, but by using symmetries of the model one can characterize them by their quantum numbers. As seen in Sec. I C, for each of the candidate phases, in the thermodynamic limit, we know the quantum numbers associated with wave functions of the (4- or 8-degenerate) ground state. Hence the relative order (in energy) of first excitations with those quantum numbers, for large enough systems, should be characteristic of the symmetry of the ground state, and thus of the phase in question. From Sec. IV A, the MCPC-1 phase is expected to extend over a finite range of W/t_2, going either to the RK point or to a nontrivial point of transition toward a RSPC phase (in analogy with the QDM on the square lattice). In Fig. 10 we plot the lowest excitation energies (in units of $\sqrt{t_2^2+W^2}$) corresponding to quantum numbers listed in Table I, as a function of the parameter $\theta=\arctan(W/t_2)$ (N.B. This is equivalent to considering the Hamiltonian $H=\sin(\theta)[H_W(W=1)]+\cos(\theta)[H_K(t_2=1)]$).

The most striking feature of these graphs concerns the states with quantum numbers $[A1,(\pi,\pi)]$ and $[B1,(0,0)]$. The excitation energy (in units of $\sqrt{t_2^2+W^2}$) of the former, being that of the charge excitation in the $\theta \to -\pi/2$ limit, collapses when θ increases. In comparison, the $[B1,(0,0)]$ state, degenerate with the ground state at $t_2=0$ (uncoupled Heisenberg chains) becomes separated energetically from the ground state when t_2 becomes non-negligible (the vanishing of both excitation energies when W/t_2 gets close to 1 is due

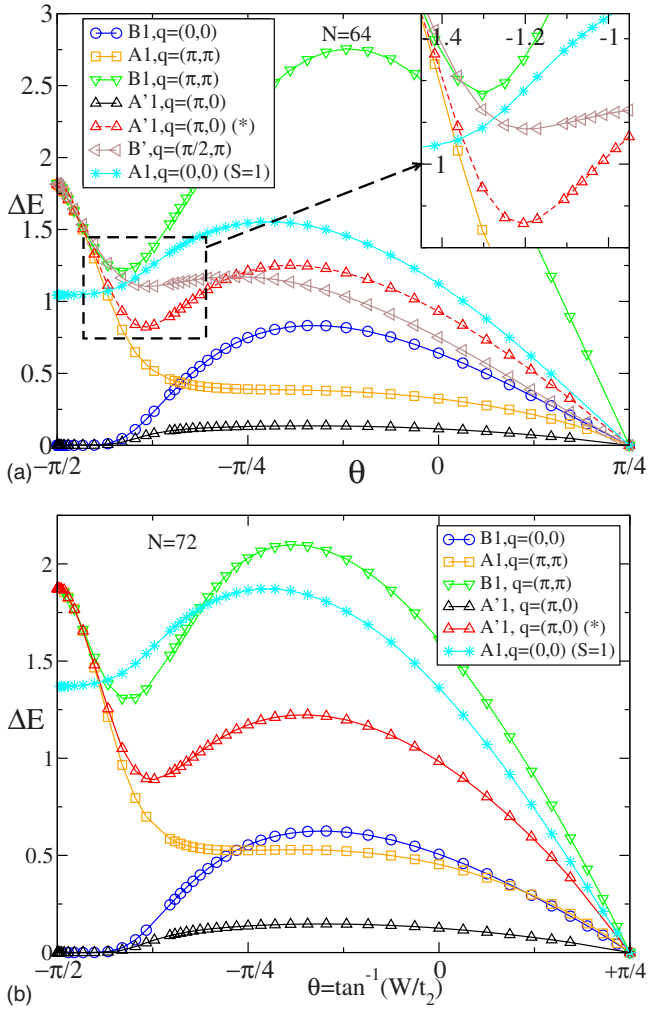

FIG. 10. (Color online) Excitation energies $\Delta E = E_{0/1} - E_{\mathrm{GS}}$ [E_1 if labeled by $(*)$] in units of $\sqrt{t_2^2+W^2}$ for different quantum numbers, in the singlet (Ref. 19) magnetic sector (open symbols) as a function of $\theta = \arctan(W/t_2)$, on the (a) $N=64$ and (b) $N=72$ checkerboard clusters. The lowest triplet excitation is also shown (star symbols).

to the degeneracy at the RK point). On the $N=64$ cluster, for a wide range of θ, the $A1,(\pi,\pi)$ state has an energy significantly lower than the $[B1,(0,0)]$ state and close to that of lowest $[A1,(0,0)]$ and $[A'1,(\pi,0)]$ states (This is less obvious with data from the $N=72$ cluster, where the effective length of chains $L=6$ results in stronger finite-size effects). The eigenvalue crossing between $[A1,(\pi,\pi)]$ and $[B1,(0,0)]$, similar to that observed for $n=1/2$, indicates a breaking or restoration of rotational symmetry, signaling a transition between the MCPC-1 phase (expected in the thermodynamic limit for $t_2 \ll |W|$) and the RSPC for which the symmetrized wave functions of the ground state have quantum numbers $[A1,(0,0)]$, $[A'1,(\pi,0)]$, $[A'1,(0,\pi)]$, and $[B1,(\pi,\pi)]$. As the data of the $N=72$ cluster are less clear, the present analysis should be extended to larger clusters, which is unrealistic with the current most advanced computational resources[20] unless we find other tools to be more conclusive about the existence and position of a MCPC-1/RSPC phase transition.

V. PLAQUETTE CORRELATIONS ON THE CHECKERBOARD

Since the finite-size effects encountered for clusters of sizes $N \leq 72$, particularly in the weak-coupling regime and at the supposed MCPC-1/RSPC transition, make it difficult to identify clearly this transition by analyzing the low-energy spectrum only, one needs complementary information about the nature of the ground state. The ED numerical technique employed in this study allows also to compute expectation values of observables and their associated correlations. Considering the structure of the different ordered phases expected in this model (both the MCPC-1 phase and the RSPC are composed of singlets localized on uncrossed plaquettes of the checkerboard), it is preferable to consider an observable defined on an uncrossed plaquette (and then symmetrized) rather than on a single site. Hence in this section we discuss results about two types of plaquette correlation functions in the ground state of the t_2-W model, computed on clusters $N=32,64,72$.

The first type of plaquette operators for which we compute correlations have $B1$ point-group symmetry, and are related to the *flippability* of a given plaquette located at $\mathbf{r}$ (i.e., of an uncrossed plaquette of the checkerboard):

$$P_-(\mathbf{r}) = (n_{1,h}n_{2,h} - n_{1,v}n_{2,v})\,\delta_{S_{1,z}+S_{2,z}}. \tag{3.1}$$

The correlations of P_- operators are computed from the ground-state wave function $|\Psi_{\mathrm{GS}}\rangle$ [first determined as the ground state in the $A1,\mathbf{q}=(0,0)$ symmetry sector and then expanded on all configurations]. The average value of P_- on the ground state being zero by symmetry (for any plaquette), the correlation function is defined as

$$C_-(R) = n_R \cdot \langle \Psi_{\mathrm{GS}} | P_-(0) P_-(\mathbf{r}) | \Psi_{\mathrm{GS}} \rangle,$$

where $P_-(0)$ is computed on a reference plaquette, $P_-(\mathbf{r})$ on a plaquette at distance R from the reference one and n_R is the number of plaquettes at distance R from the reference. A nonzero value of $C_-(R)$ in the thermodynamic limit and at large distances corresponds to a phase breaking the $\pi/2$-rotational symmetry (hence in this context to the MCPC-1 phase).

In Fig. 11 are shown, for each of the cluster sizes considered, correlations $C_\alpha(R=d_{\max})$ at the maximal distance between plaquettes equivalently occupied in a *plaquette* phase ($d_{\max}=2\sqrt{2}$ for $N=32,72$ and $d_{\max}=4$ for $N=64$). We also plot Fourier transforms S_- of C_- correlations, for wave vectors $\mathbf{q}=(0,0)$ and $\mathbf{q}=(\pi,\pi)$. These Fourier transforms are computed with a truncation at short distances; i.e., only correlations for distances $r \geq 2$ are taken into account (distances $R=0,1$ are discarded since the plaquette operators on neighboring plaquettes share at least one site; at distance $R=\sqrt{2}$ the simultaneous double occupancy of both plaquettes is forbidden by the *dimer constraint*).

The correlations of the $B1$ plaquette operator (P_-) vary significantly with θ between the Heisenberg and the RK limits, and give important information about the evolution of the ground state. Correlations of P_- decrease strongly for $\theta \leq -3\pi/8$ (which means $W/t_2 \leq W_c \sim -2.4$), both at the largest distance $d_{\max}$ between equivalent plaquettes, and in

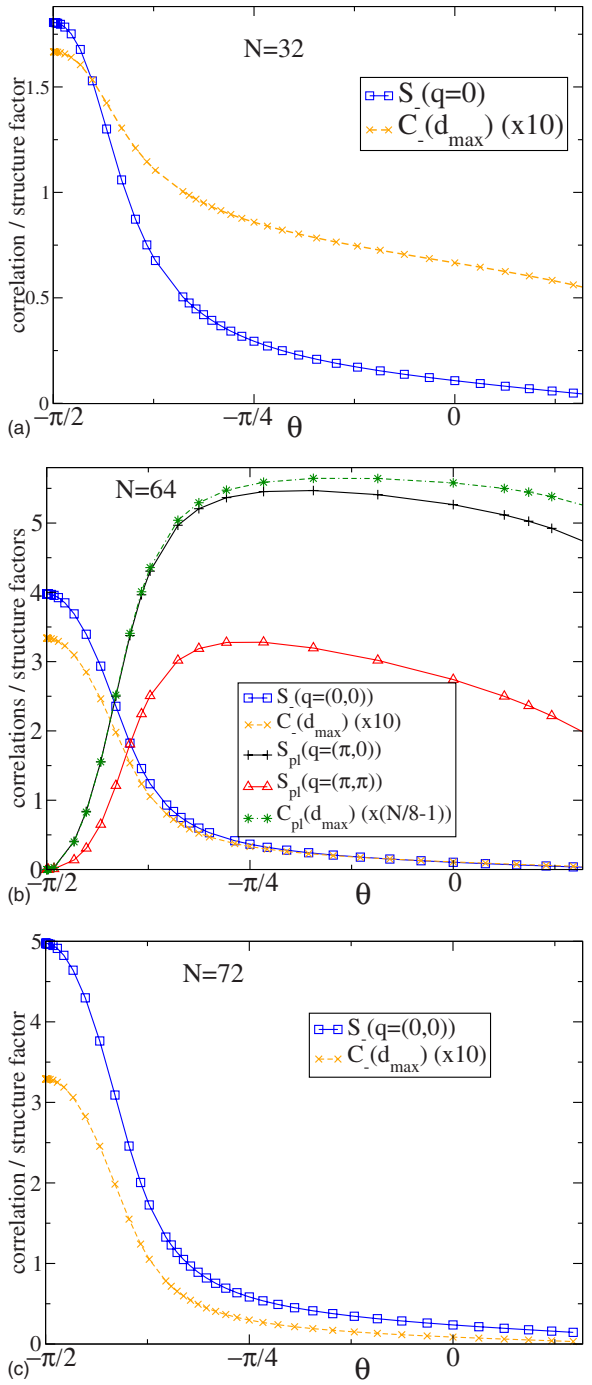

FIG. 11. (Color online) Correlations in real space (C_-) at distance $d_{\max}$ (dashed and dotted curves), and in reciprocal space (S_-) at $\mathbf{q}=0$ (square symbols) of $B1$ plaquette operators, on clusters of size (a) $N=32$, (b) $N=64$, and (c) $N=72$, as a function of $\theta=\arctan(W/t_2)$. On graph (b) are also shown, for the $N=64$ cluster, plaquette-exchange correlations $C_{\rm pl}$ at distance $d_{\max}$ and the corresponding structure factor $S_{\rm pl}$ at $\mathbf{q}=(\pi,0)$ and $\mathbf{q}=(\pi,\pi)$.

Fourier space at wave vector $\mathbf{q}=(0,0)$—in the weak-coupling regime [for $\theta\leq\theta_c\sim-1.2(1)$] $S_-[\mathbf{q}=(0,0)]$ is well approximated by a Gaussian function of $\theta+\pi/2$; for $\theta\geq\theta_c$, the ratio $S_-(\theta)/S_-(-\pi/2)$ becomes smaller when $d_{\max}$ increases, so one can expect $B1$ plaquette correlations to vanish in the thermodynamic limit. This indicates that the rotational symmetry of the lattice, broken in the weak-coupling regime, is restored for $\theta\geq\theta_c$, which is a signature of a transition to a RSPC phase.

We also computed (off-diagonal) plaquette-exchange correlations, i.e., correlations of the kinetic operator

$$P_{\square}(r)=(b^{\dagger}_{i\uparrow}b^{\dagger}_{j\downarrow}+b^{\dagger}_{i\downarrow}b^{\dagger}_{j\uparrow})(b_{k\uparrow}b_{l\downarrow}+b_{k\downarrow}b_{l\uparrow})+\text{c.c.}$$

(where sites i, j, k, l are those around the void plaquette at position r). The connected correlations $C_{\rm pl}(r)=\langle P_{\square}(r)P_{\square}(0)\rangle-\langle P_{\square}(0)\rangle^2$ are vanishing in the $\theta\to-\pi/2$ limit, where charge moves away from Heisenberg chains are energetically forbidden; on the contrary, in a RSPC, they are expected to be important between *resonating plaquettes* [at relative position $(2p,2q)-p$, $q\in\mathbb{Z}$ from each other] and significantly smaller otherwise. Consequently we focus specifically on plaquette-exchange structure factors $S_{\rm pl}(\mathbf{q})$ (Fourier transforms of the corresponding correlations) at $\mathbf{q}=(\pi,0)$, $\mathbf{q}=(0,\pi)$, and $\mathbf{q}=(\pi,\pi)$. They are shown for the $N=64$ cluster, along with the correlation in real space at maximal distance $C_{\rm pl}(d_{\max})$, in Fig. 11 [graph (b)].

These correlations increase significantly with θ in the weak-coupling regime, indicating the appearance of resonating plaquettes characterizing the MCPC-1 and RSPC phases. We have checked (not shown) that the $(\pi,0)$ structure factor is very well approximated by its contribution from correlations between resonating plaquettes only, which indicates that the picture of a *plaquette pattern* describes well the ground-state wave function at $\theta\geq\theta_c$, where these correlations are important. The smaller value of the structure factor at $\mathbf{q}=(\pi,\pi)$ compared to that at $\mathbf{q}=(\pi,0)$ originates from non-negligible correlations at short distances such as $d=\sqrt{5}$. The comparison between the correlation $C_{\rm pl}(d_{\max})$ rescaled by a factor $N/8-1$ (accounting for the number of plaquettes included in the Fourier sum defining $S_{\rm pl}$ and that should be occupied and resonating in a MCPC-1 or RSPC phase, and the structure factor $S_{\rm pl}(\pi,0)$ itself, is eloquent: it indicates that for $\theta\leq\theta_c$, almost all contributions to the Fourier transform come from resonating plaquettes, and the correlations between these plaquettes are long ranged. For larger values of θ $(\geq\theta_c)$ the (negative) contributions from other plaquettes become non-negligible; but structure factors at both wave vectors remain significant, and indicate the robustness of the ordering on these plaquettes. Although plaquette-exchange correlations alone are not sufficient to distinguish the RSPC from the MCPC-1 phase, their change in behavior around $\theta=\theta_c$, associated with features of the low-energy spectrum and $B1$ (diagonal) plaquette correlations, indicates the presence of a MCPC-1/RSPC phase transition (Fig. 12).

VI. CONCLUSION AND PERSPECTIVES

In summary, we have considered $S=1/2$ fermions on the checkerboard lattice, with an extended Hubbard model in a limit of infinite on-site and strong nearest-neighbor Coulomb repulsions, at the specific fractional 1/8 filling. In this limit, constraints characteristic of the square lattice dimer model naturally emerge, with the links on the square lattice corresponding to the sites of the checkerboard. Moreover, the lowest-order kinetic process allowed in perturbation (from

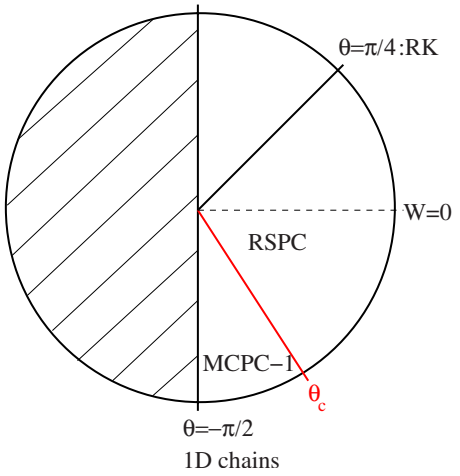

FIG. 12. (Color online) Phase diagram of the t_2-W model of $S=1/2$ fermions at $n=1/4$ [in the range of parameter $-\pi/2 \leq \theta \leq \pi/4$ where $\theta=-\arctan(W/t_2)$]. The MCPC-1/RSPC transition occurs at $\theta_c \sim -3\pi/8 \pm 0.2$ according to exact diagonalization results [a value $\theta_c=\arctan(-4)$ is estimated variationally].

the infinite repulsion limit) flips two particles around an uncrossed plaquette, recalling the kinetic term of the quantum dimer model, and the analogy is reinforced by considering an extra term similar to the potential term of the QDM. However, here the spin degrees of freedom of particles play an essential role, since kinetic processes act only on singlet states on a plaquette. The model we have considered makes a continuous connection between the physics of critical Heisenberg chains (occurring in place of the *columnar* limit of the QDM) and a RK-*type* critical point of the present model.

Starting from a situation where the Heisenberg chains of the first case are weakly coupled, we have identified the leading order—in perturbation in t_2/W—term coupling neighboring chains, and characterized it as a relevant perturbation for the Heisenberg chains, driving their in-phase dimerization in the thermodynamic limit as soon as the coupling is finite. The corresponding phase (*mixed columnar-plaquette crystal-1*) distinguishes itself from other candidate phases (RSPC and *columnar*) of the model by a lower symmetry, and its extent in parameter space is determined by a detailed analysis of the low-energy spectrum obtained by exact diagonalization, taking lattice and time reversal symmetries into account. This analysis indicates that, when going toward the RK-type point, the MCPC-1 phase persists up to a transition into a $\pi/2$-rotational invariant *resonating singlet-pair crystal*, the analog of the plaquette phase of the square lattice QDM; this transition is confirmed by the computation of various types of correlations between uncrossed plaquettes of the checkerboard, characterizing the plaquette ordering, and the symmetries of the ground state. The qualitative features of this phase diagram are also found by a variational approach, also indicating that the transition between the MCPC-1 phase and RSPC should be of second order. In particular, the system described by the extended-Hubbard model with strong repulsions considered first appears to be in a *resonating singlet-pair crystal*, similarly to the corresponding model at quarter filling.[9]

An open question is to know what happens at small but finite doping from the 1/8 filled case: a possibility is that the system remains in a crystalline phase confining the doping particles (either holes or electrons depending on the type of doping); alternatively, the RSPC could give way to a phase with either deconfined doping particles or the formation of bound Cooper pairs (as it happens in systems at small doping from 1/4 filling and 1/2 filling[21]) that would be an indication of a superconducting or supersolid phase.

ACKNOWLEDGMENTS

F.T. and D.P. thank S. Capponi for discussions on the two-coupled chain problem, the French Research Council (ANR) for financial support, and IDRIS (Orsay, France) for computation time. Likewise, R.M. thanks Oleg Starykh for explanations of his related work. R.M. and D.P. thank the Kavli Institute for Theoretical Physics, where this collaboration was initiated, for hospitality.

[1] B. Canals and C. Lacroix, Phys. Rev. Lett. **80**, 2933 (1998).
[2] J.-B. Fouet, M. Mambrini, P. Sindzingre, and C. Lhuillier, Phys. Rev. B **67**, 054411 (2003); R. Moessner, O. Tchernyshyov, and S. L. Sondhi, J. Stat. Phys. **116**, 755 (2004).
[3] S. Wessel and M. Troyer, Phys. Rev. Lett. **95**, 127205 (2005); D. Heidarian and K. Damle, *ibid.* **95**, 127206 (2005); R. G. Melko, A. Paramekanti, A. A. Burkov, A. Vishwanath, D. N. Sheng, and L. Balents, *ibid.* **95**, 127207 (2005); A. Sen, P. Dutt, K. Damle, and R. Moessner, *ibid.* **100**, 147204 (2008).
[4] A. Sen, K. Damle, and T. Senthil, Phys. Rev. B **76**, 235107 (2007).
[5] F. Pollmann, J. J. Betouras, K. Shtengel, and P. Fulde, Phys. Rev. Lett. **97**, 170407 (2006); F. Pollmann, P. Fulde, and E. Runge, Phys. Rev. B **73**, 125121 (2006).
[6] P. Fulde, K. Penc, and N. Shannon, Ann. Phys. **11**, 892 (2002).
[7] D. S. Rokhsar and S. A. Kivelson, Phys. Rev. Lett. **61**, 2376 (1988).
[8] R. Moessner and S. L. Sondhi, Phys. Rev. B **68**, 054405 (2003).
[9] D. Poilblanc, K. Penc, and N. Shannon, Phys. Rev. B **75**, 220503(R) (2007).
[10] D. Poilblanc, Phys. Rev. B **76**, 115104(R) (2007).
[11] S. Wessel, Phys. Rev. B **78**, 075112 (2008).
[12] M. Indergand, C. Honerkamp, A. Läuchli, D. Poilblanc, and M. Sigrist, Phys. Rev. B **75**, 045105 (2007).
[13] A. Ralko, D. Poilblanc, and R. Moessner, Phys. Rev. Lett. **100**, 037201 (2008).
[14] For an $N=72$ cluster with PBC, the Hilbert space, as defined previously (using spin inversion, point-group symmetries, and translations keeping invariant each sublattice of the dimer lattice) in the most symmetric sector $(A1, \mathbf{q}=0)$ has 192 790 configurations; for $t_2=1$ and $W=-2$, the energy of the ground state is $E_{GS}=-62.63747973...$

[15] O. A. Starykh, A. Furusaki, and L. Balents, Phys. Rev. B **72**, 094416 (2005).

[16] F. H. L. Essler, A. M. Tsvelik, and G. Delfino, Phys. Rev. B **56**, 11001 (1997).

[17] For the $W=0$ case (derived from the extended Hubbard model), the energy per particle of the RSPC (and MCPC-2) variational wave function in units of t_2 is $E=-1$, while the exact values on periodic clusters are respectively $N=32$, 48, 64 and 72 are respectively (given with 0.001 precision): $-1.166; -1.136; -1.088; -1.099$. (The two last clusters being oriented at $\pi/4$ from each other, the relative position of their ground-state energies is not anormal). A rough estimate would give $E=-1.06(2)$ in the thermodynamic limit.

[18] Close to $W=t_2$ and in the thermodynamic limit, the RK wave function has an energy of $2(W-t_2)n_{\mathrm{fl}}$ per uncrossed plaquette (so twice as much per particle), where n_{fl}, the probability for a given plaquette to be flippable, equals 1/4. Similarly, in the bosonic case, the flippability is $n_{\mathrm{fl}}=1/4$ and the energy of the RK state equals $(V-t)/2$ per particle.

[19] Using the spin inversion symmetry allows one to compute eigenstates and eigenenergies in sectors of total spin either odd or even, but not explicitly in the $S=0$ or $S=1$ sector. However it is known that states of lowest energy are of total spin $S=0$ or $S=1$.

[20] Two clusters of size $N=80$ would be tractable by exact diagonalization, but there either the $\pi/2$ rotation symmetry or the reflexion symmetry would be lost (in comparison to the $N=64$ cluster for instance) which would be problematic for determining the quantum numbers characterizing the phases of the model. The next cluster available (by increasing N) and possessing these symmetries would be the $N=128$ cluster, far beyond the limits of existing numerical resources for exact diagonalizations.

[21] D. Poilblanc, Phys. Rev. Lett. **93**, 197204 (2004).